

Supporting Information

A simple fabrication of carbaldehyde based fluorescent “turn-on” probe for the selective and sole detection of Pd²⁺: Application as test strips

Chandan Kumar Manna, Saswati Gharami, Krishnendu Aich, Lakshman Patra and Tapan K. Mondal

Department of Chemistry, Jadavpur University, Kolkata-700032

E-mail: tapank.mondal@jadavpuruniversity.in

CONTENTS

Fig. S1. ¹H-NMR spectrum of DHMC

Fig. S2. ¹³C-NMR spectrum of DHMC

Fig. S3. HRMS spectrum of DHMC

Fig. S4. HRMS spectrum of DHMC-Pd²⁺

Fig. S5. Change in UV-Vis spectra of the probe (DHMC) (10 μM) upon addition of 2 equivalent of various metal ions (10 μM)

Fig. S6. Change in emission spectra of the probe (DHMC) (10 μM) upon addition of 2 equivalent of various metal ions (10 μM)

Fig. S7. Job's plot of DHMC for Pd²⁺

Fig. S8. Linear response curve of DHMC depending on Pd²⁺ concentration

Fig. S9. Mole ratio plot of DHMC for Pd²⁺

Fig. S10. Determination of association constant of DHMC for Pd²⁺ from fluorescence titration data

Fig. S11. Lifetime decay profile of DHMC and DHMC-Pd²⁺

Fig. S12. pH study of DHMC for Pd²⁺

Fig. S13. X-ray Data Collection and Crystal Structure Determination of the probe (DHMC)

Fig. S14. Contour plots of some selected molecular orbitals of DHMC

Fig. S15. Contour plots of some selected molecular orbitals of DHMC-Pd²⁺

Fig. S16. Optimized structure of DHMC calculated by DFT/B3LYP/6-31+G(d) method

Fig. S17. Optimized structure of DHMC-Pd²⁺ calculated by DFT/B3LYP/6-31+G(d) method

Fig. S18. Determination of emission quantum yield (Φ) of DHMC and its complex with Pd²⁺

Table S1. Crystallographic data and refinement parameters of the DHMC

Table S2. Selected X-ray and calculated bond distances and angles of DHMC

Table S3. Energy and compositions of some selected molecular orbitals of DHMC - Pd²⁺

Table S4. Vertical electronic transitions calculated by TDDFT/B3LYP/CPCM method for DHMC and DHMC-Pd²⁺ in acetonitrile

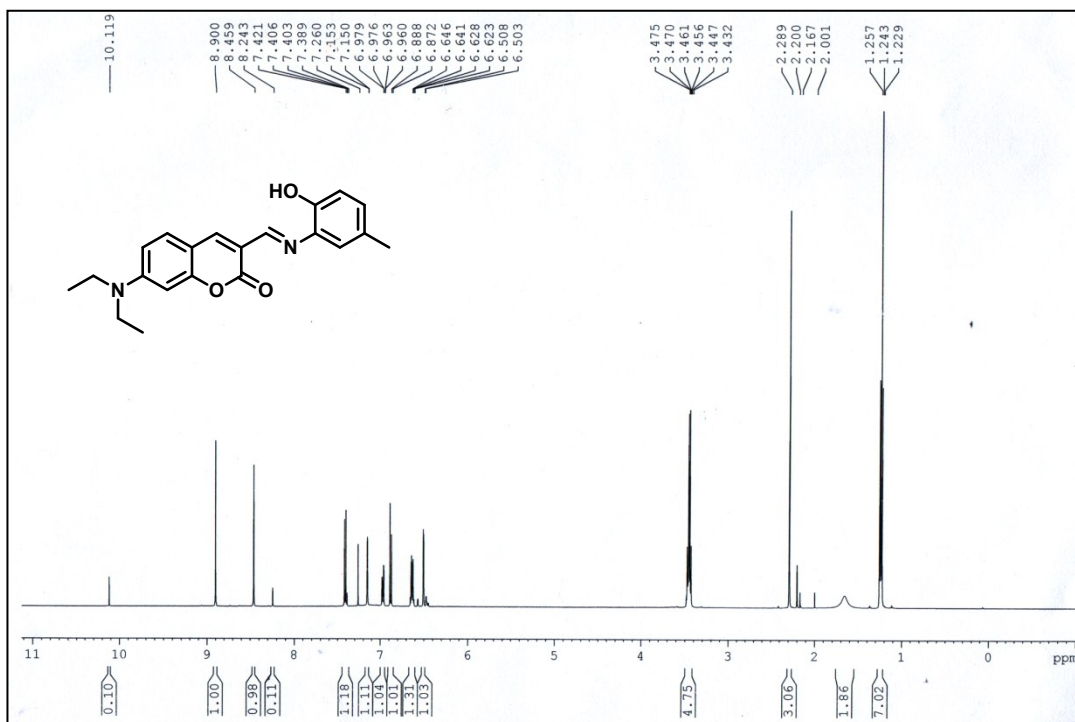


Figure S1: ^1H NMR (300 MHz) spectrum of the probe (DHMC) in CDCl_3

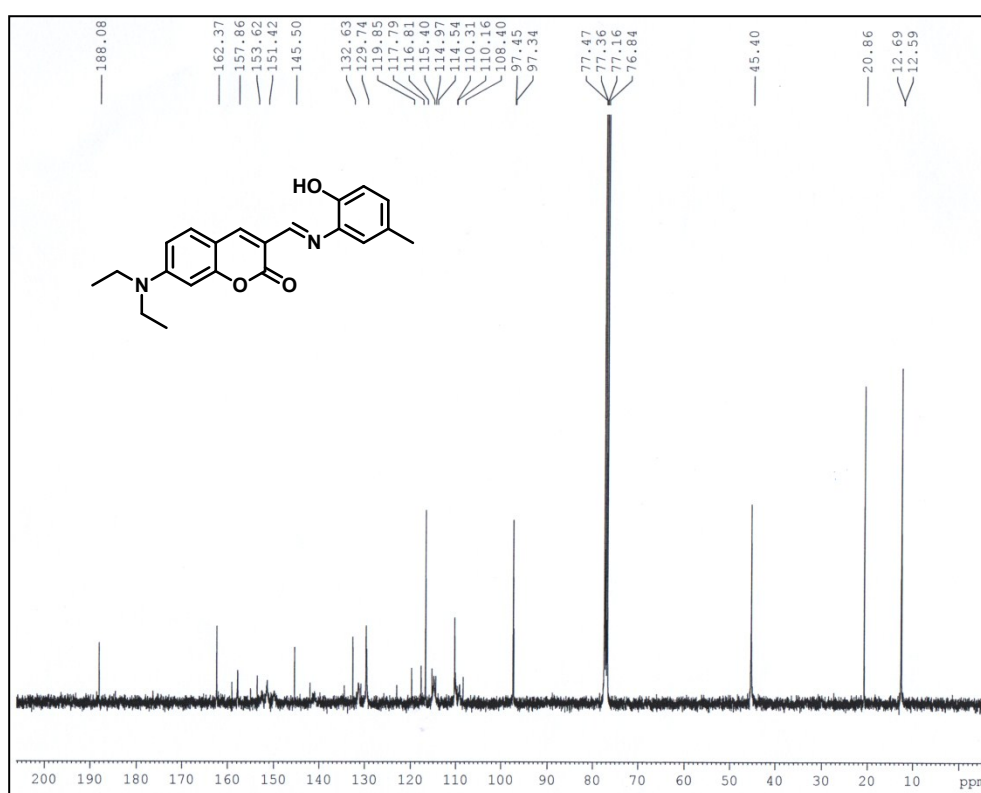


Figure S2: ^{13}C NMR (75 MHz) spectrum of the probe (DHMC) in CDCl_3

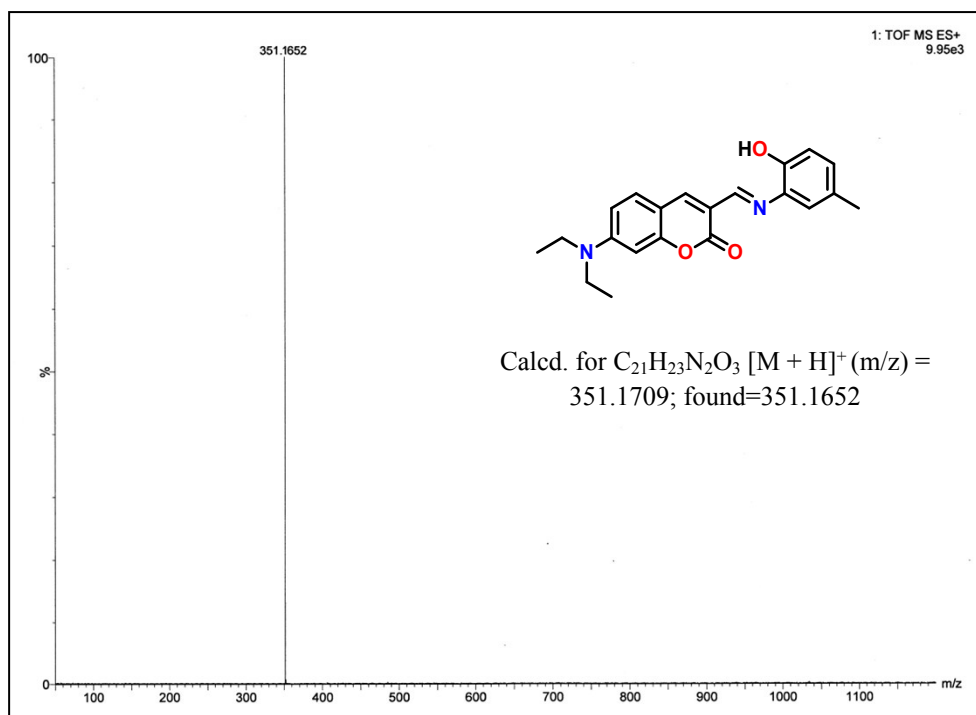


Figure S3: HRMS of the probe (DHMC)

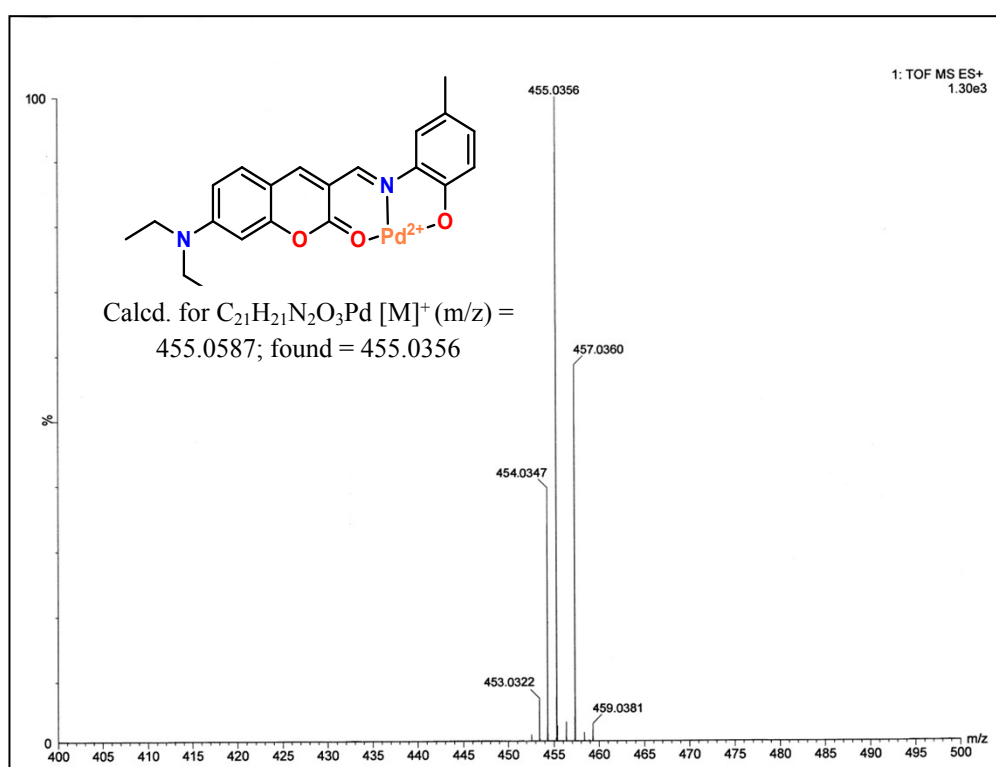


Figure S4: HRMS spectrum of DHMC- Pd^{2+}

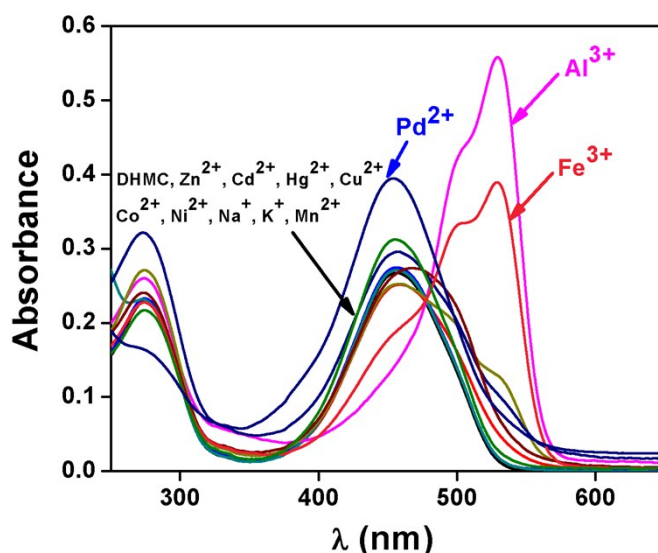


Figure S5: UV-vis change of DHMC (10 μM) upon addition of different metal ions, i.e., Na^+ , K^+ , Ca^{2+} , Mg^{2+} , Mn^{2+} , Fe^{3+} , Al^{3+} , Cr^{3+} , Co^{2+} , Ni^{2+} , Hg^{2+} , Zn^{2+} , Cu^{2+} , Pb^{2+} and Cd^{2+} (40 μM) in $\text{CH}_3\text{CN}/\text{H}_2\text{O}$ (4/1, v/v) using HEPES buffered solution at $\text{pH}=7.2$.

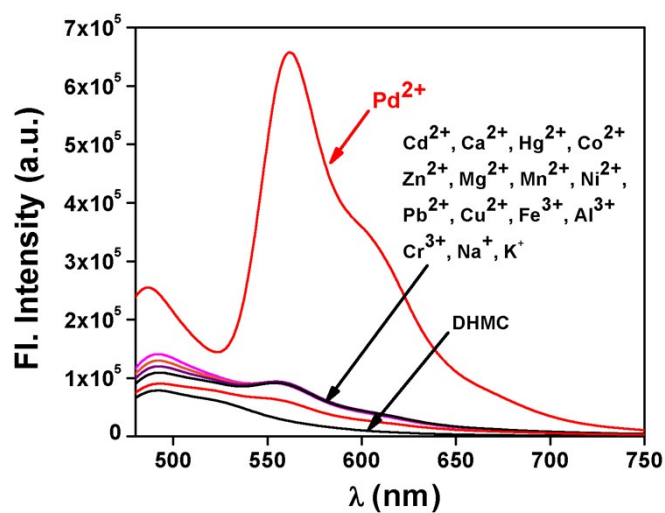


Figure S6: Change in emission intensity of DHMC (10 μM) upon addition of different metal ions, i.e., Na^+ , K^+ , Ca^{2+} , Mg^{2+} , Mn^{2+} , Fe^{3+} , Cr^{3+} , Al^{3+} , Co^{2+} , Ni^{2+} , Hg^{2+} , Zn^{2+} , Cu^{2+} , Pb^{2+} and Cd^{2+} (40 μM) in $\text{CH}_3\text{CN}/\text{H}_2\text{O}$ (4/1, v/v) using HEPES buffered solution at $\text{pH}=7.2$.

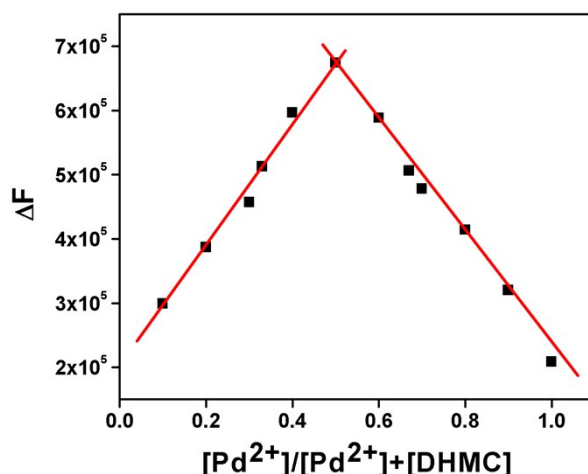


Figure S7: Job's plot of DHMC for Pd²⁺

Determination of detection limit:

The detection limit was calculated based on the fluorescence titration. To determine the S/N ratio, the emission intensity of DHMC without Pd²⁺ was calculated by 10 times and the standard deviation of blank measurements was determined. The detection limit of **DHMC** for Pd²⁺ was determined from the following equation¹:

$$DL = K \times Sb_1/S$$

Where K = 2 or 3 (we take 3 in this case); Sb₁ is the standard deviation of the blank solution; S is the slope of the calibration curve.

From the graph we get slope = 4.96 × 10¹⁰ and Sb₁ value is 1226.2888

Thus using the formula we get the Detection Limit = 7.41 × 10⁻⁸ M i.e., DHMC can detect Pd²⁺ in this minimum concentration through fluorescence techniques.

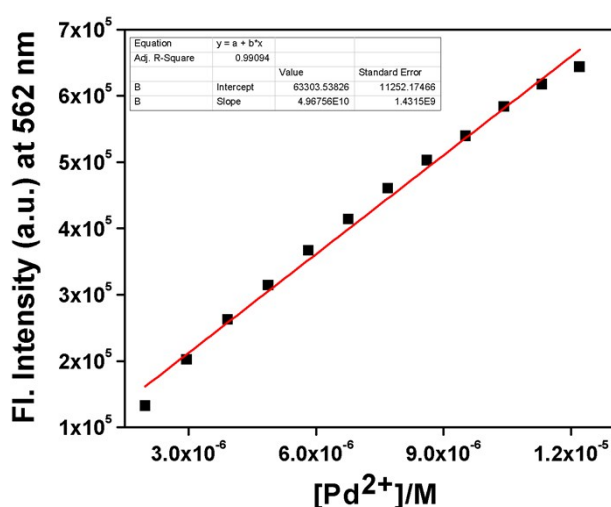


Figure S8: Linear response curve of DHMC at 562 nm depending on the Pd²⁺ concentration

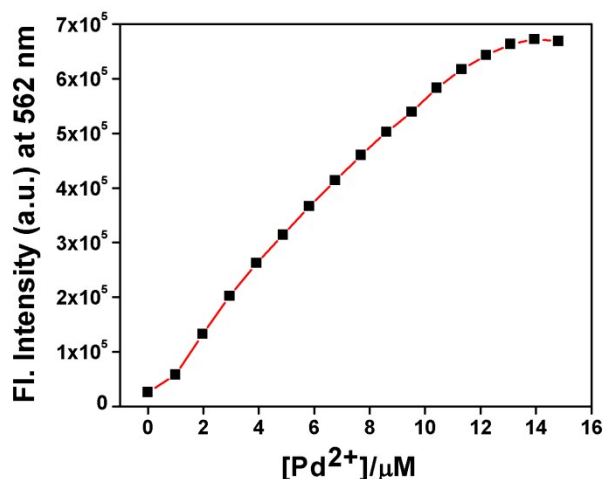


Figure S9: Mole ratio plot of DHMC for Pd²⁺

Determination of binding constant from Fluorescence titration data:

Binding constant was calculated according to the Benesi-Hildebrand equation. K_a was calculated following the equation stated below.

$$1/(F-F_0) = 1/\{K_a(F_{max}-F_0) [M^{n+}]^x\} + 1/[F_{max}-F_0]$$

Here F_0 , F and F_{max} indicate the emission in absence of, at intermediate and at infinite concentration of metal ion respectively.

Plot of $1/[F-F_0]$ vs $1/[Pd^{2+}]$ gives a straight line indicating 1:1 complexation between DHMC and Pd²⁺ where K_a is found to be $1.69 \times 10^5 \text{ M}^{-1}$ for DHMC.

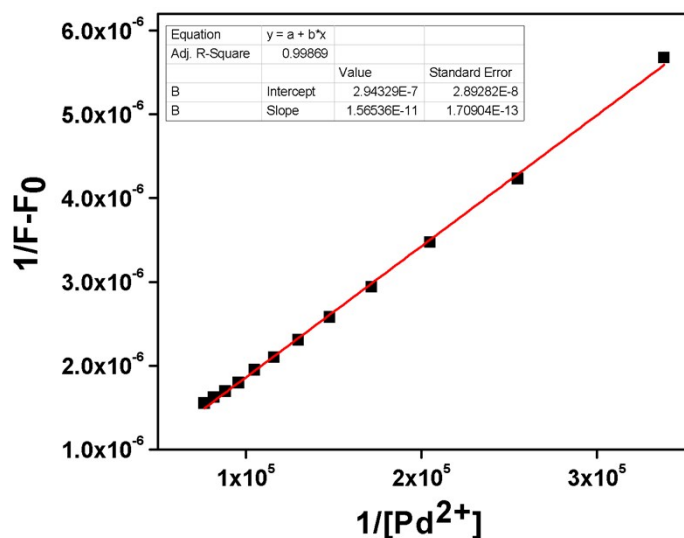


Figure S10: Determination of association constant of DHMC at 562 nm depending on the Pd²⁺ concentration using Benesi-Hildebrand equation

Determination of fluorescence Quantum Yields (Φ) of DHMC and its complex with Pd²⁺

The luminescence quantum yield was determined using fluorescein ($\phi_s = 0.924$ in 0.1M NaOH) as reference dye. The compounds and the reference dye were excited at the same wavelength and the emission spectra were recorded. The area of the emission spectrum was integrated and the quantum yield is calculated according to the following equation:

$$\Phi_x = \Phi_s \times \left(\frac{I_x}{I_s}\right) \times \left(\frac{A_s}{A_x}\right) \times \left(\frac{n_x}{n_s}\right)^2$$

Where, x & s indicate the unknown and standard solution respectively, ϕ is the quantum yield, I is the integrated area under the fluorescence spectra, A is the absorbance and n is the refractive index of the solvent.

The quantum yields of DHMC and DHMC-Pd²⁺ are determined using the above mentioned equation and the values are found to be 0.01 and 0.12 respectively.

Lifetime study:

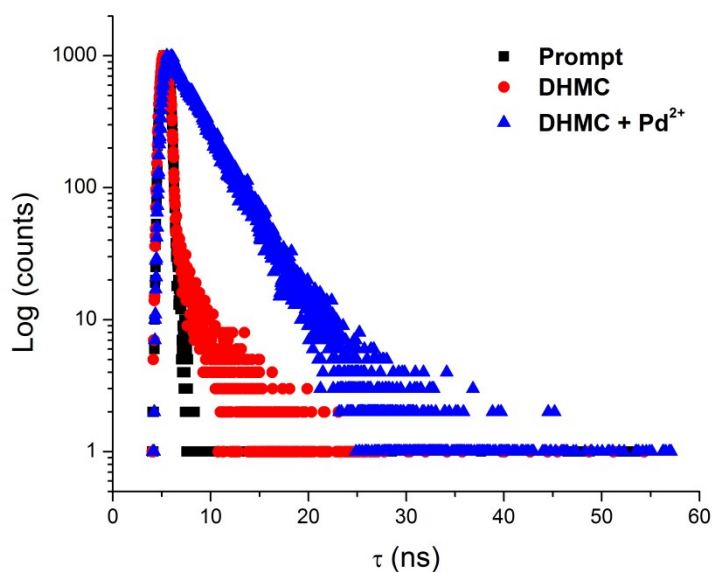


Figure S11: Lifetime decay profile of DHMC ($\tau_{av} = 0.536$ ns) and DHMC-Pd²⁺ ($\tau_{av} = 3.156$ ns)

pH study:

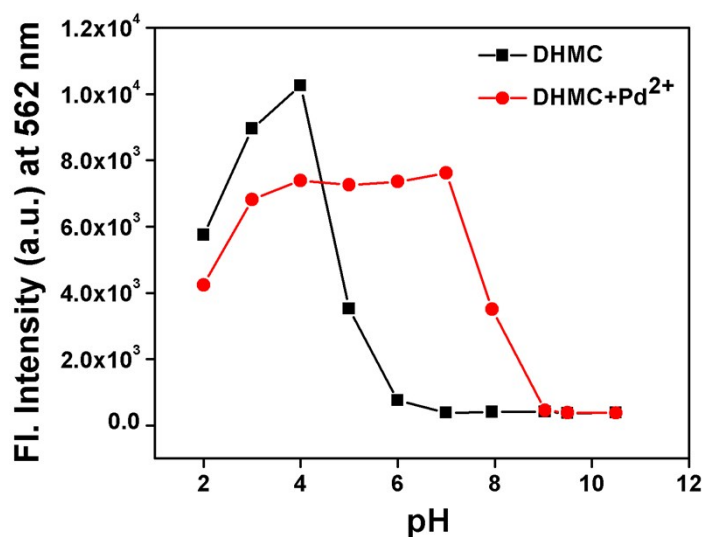


Figure S12: pH study of DHMC for Pd²⁺

X-ray Data Collection and Crystal Structure Determination of the probe (DHMC):

Single crystals of DHMC were obtained by slow diffusion of *n*-hexane into dichloromethane solution of the compound. X-ray data were collected using an automated Bruker SC-XRD single crystal X-ray diffractometer equipped with a Bruker D8 - QUEST detector using a fine focus sealed tube as the radiation source of graphite monochromated MoK α radiation ($\lambda = 0.71073 \text{ \AA}$). Details of crystal analyses, data collection and structure refinement are summarized in Table S3. Reflection data were recorded using the ω scan technique. The structure was solved by direct method using SHELXT 2014/5 (Sheldrick, 2014) and refined by full matrix least squares technique on F2 using anisotropic displacement parameters for all non-hydrogen atoms using SHELXL-2016/6 (Sheldrick, 2016). Hydrogen atoms were included in the refinement process as per the riding model. Crystallographic data have been deposited at the Cambridge Crystallographic Data Centre with CCDC 1939357 for DHMC. Copies of the data can be obtained free of charge on application to the CCDC, 12 Union Road, Cambridge CB2 IEZ, UK. Fax: +44-(0)1223-336033 or e-mail:deposit@ccdc.cam.ac.uk.

Table S1. Crystallographic data and refinement parameters of the probe (DHMC)

Formula	C ₂₁ H ₂₂ N ₂ O ₃
Formula Weight	350.40
Crystal System	triclinic
Space group	<i>P</i> -1
a, b, c [Å]	6.8046(5), 9.5931(8), 14.6934(12)
α	95.313(3)
β	102.442(2)
γ	105.848(3)
V [Å ³]	889.23(12)
Z	2
D(calc) [g/cm ³]	1.309
Mu(MoKa) [/mm]	0.088
F(000)	372
Temperature (K)	293(2)
Radiation [Å]	0.71073
θ (Min-Max) [°]	2.236-27.052
Dataset (h; k; l)	-8 to 8; -12 to 12; -18 to 18
Total, Unique Data, R(int)	30086/3853/0.0369
R, wR ₂	0.0495, 0.1363
Goodness of fit(S)	1.042
CCDC No.	1939357

Table S2. Selected X-ray and calculated bond distances and angles of DHMC

Bonds(Å)	X-ray	Calc.
O(1)-C(1)	1.360(2)	1.35448
O(2)-C(10)	1.2037(19)	1.21035
O(3)-C(11)	1.3759(18)	1.36416
O(3)-C(10)	1.3890(19)	1.39679
N(1)-C(8)	1.267(2)	1.28789
N(1)-C(7)	1.408(2)	1.40171
N(2)-C(15)	1.371(2)	1.37819

N(2)-C(18)	1.449(2)	1.46525
N(2)-C(20)	1.457(2)	1.46486
Angles(°)	X-ray	Calc.
C(1)-O(1)-H(1)	110(2)	104.11144
C(11)-O(3)-C(10)	122.70(12)	123.14884
C(8)-N(1)-C(7)	122.32(14)	122.82897
C(15)-N(2)-C(18)	120.98(15)	120.92458
C(15)-N(2)-C(20)	121.75(15)	121.25880
C(18)-N(2)-C(20)	116.92(14)	117.73503
O(1)-C(1)-C(2)	119.39(16)	120.12546
O(1)-C(1)-C(7)	120.34(15)	119.71478
C(2)-C(1)-C(7)	120.28(17)	120.15913
C(3)-C(2)-C(1)	120.33(18)	119.59070

Theoretical study:

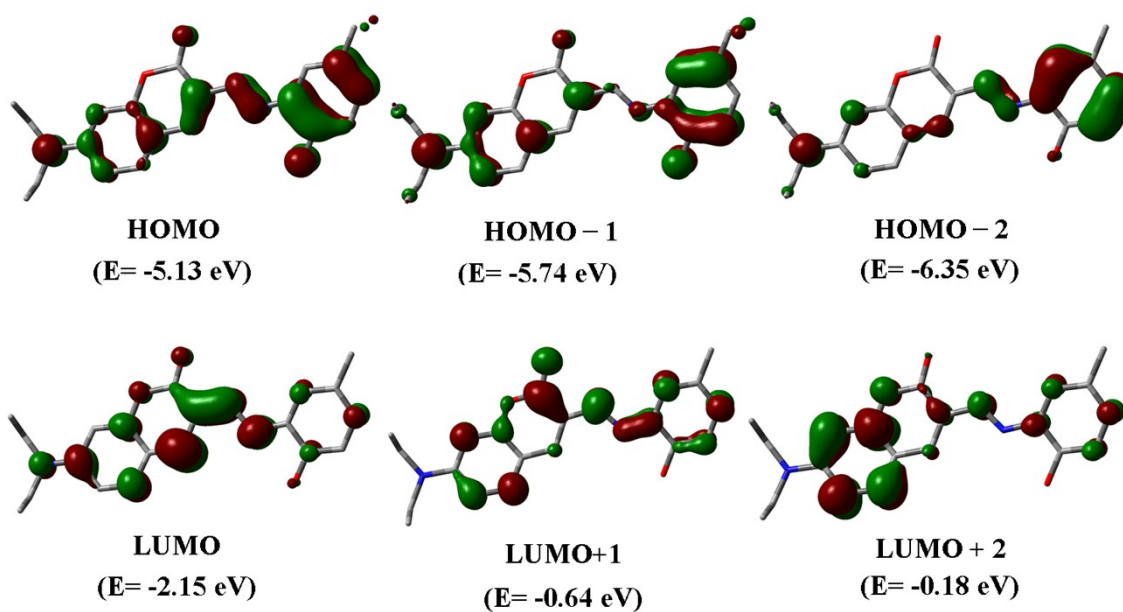


Figure S13. Contour plots of some selected molecular orbitals of DHMC

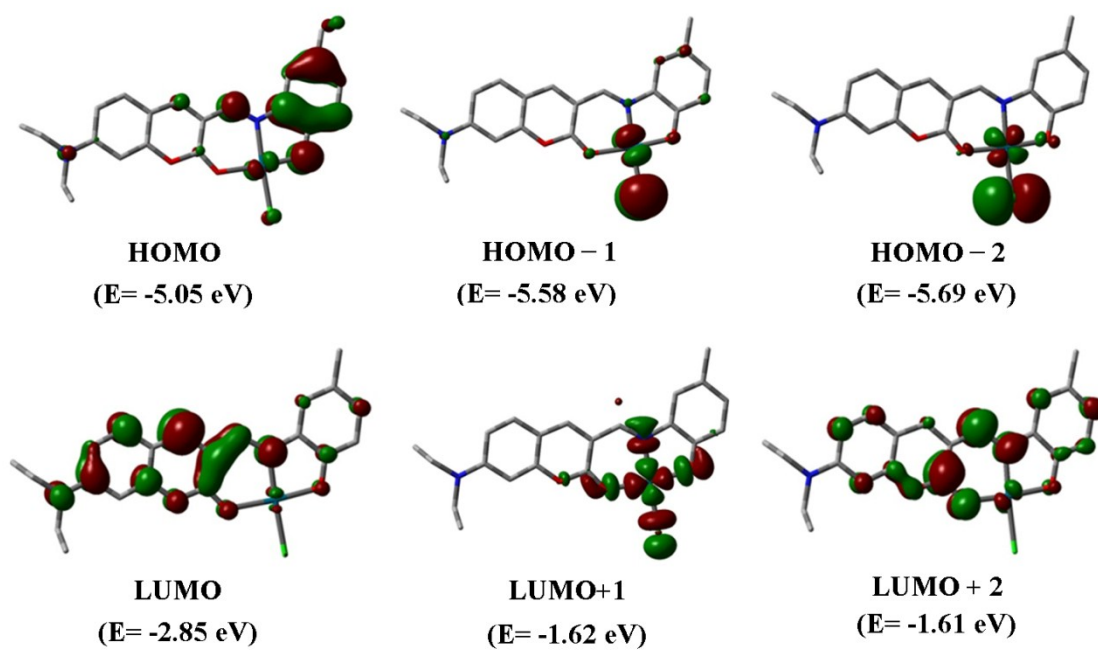


Figure S14. Contour plots of some selected molecular orbitals of DHMC-Pd²⁺

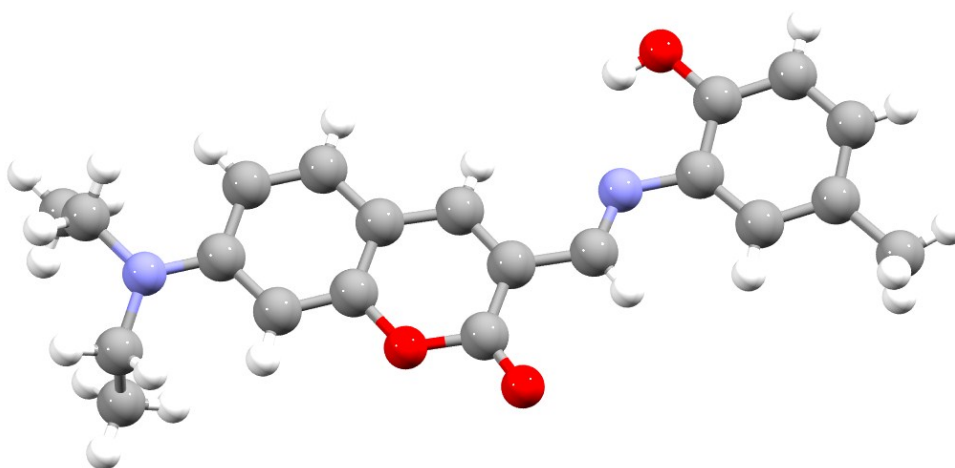


Figure S15. Optimized structure of DHMC calculated by DFT/B3LYP/6-31+G(d) method

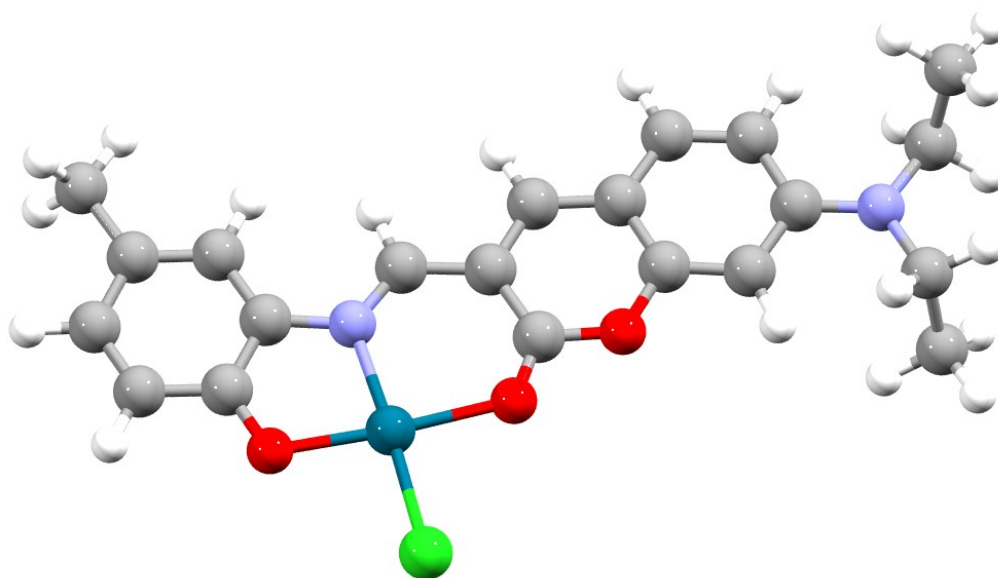


Figure S16. Optimized structure of DHMC-Pd²⁺ calculated by DFT/B3LYP/6-31+G(d) method

Table S3. Energy and compositions of some selected molecular orbitals of DHMC-Pd²⁺

MO	Energy (eV)	% of composition		
		Pd	DHMC	Cl
LUMO+5	0.33	100	0	1
LUMO+4	-0.36	1	99	0
LUMO+3	-0.88	0	100	0
LUMO+2	-1.61	3	97	0
LUMO+1	-1.62	56	30	15
LUMO	-2.85	2	98	1
HOMO	-5.05	4	93	2
HOMO-1	-5.58	25	14	61
HOMO-2	-5.69	16	2	82
HOMO-3	-6.08	10	80	10
HOMO-4	-6.16	79	11	10
HOMO-5	-6.72	5	95	0
HOMO-6	-6.86	53	46	0
HOMO-7	-7.3	35	54	11
HOMO-8	-7.43	18	24	57
HOMO-9	-7.52	61	17	21
HOMO-10	-7.66	6	94	0

Table S4. Vertical electronic transitions calculated by TDDFT/B3LYP/CPCM method for DHMC and DHMC-Pd²⁺ in acetonitrile

Compds.	Energy (eV)	Wavelength (nm)	Osc. strength (f)	Transition	Character
DHMC	2.6769	463.1	1.1811	(98%) HOMO→LUMO	$\pi(\text{L}) \rightarrow \pi^*(\text{L})$
	3.2388	382.8	0.1379	(95%) HOMO-1→LUMO	$\pi(\text{L}) \rightarrow \pi^*(\text{L})$
	3.7959	326.6	0.0096	(66%) HOMO-2→LUMO	$\pi(\text{L}) \rightarrow \pi^*(\text{L})$
	3.8947	318.3	0.0058	(77%) HOMO-3→LUMO	$\pi(\text{L}) \rightarrow \pi^*(\text{L})$
	3.9921	310.5	0.1219	(74%) HOMO→LUMO+1	$\pi(\text{L}) \rightarrow \pi^*(\text{L})$
DHMC-Pd ²⁺	2.2985	539.4	0.4888	(95%) HOMO→LUMO	$\pi(\text{L}) \rightarrow \pi^*(\text{L})$
	2.7246	455.0	0.0966	(89%) HOMO-3→LUMO	$\pi(\text{L}) \rightarrow \pi^*(\text{L})$
	2.9006	427.4	0.7783	(88%) HOMO-1→LUMO	$p\pi(\text{Cl}) \rightarrow \pi^*(\text{L})$
	2.9963	413.8	0.0014	(79%) HOMO-5→LUMO+1	$\pi(\text{L}) \rightarrow d\pi(\text{Pd})$
	3.1928	388.3	0.1302	(86%) HOMO→LUMO+3	$\pi(\text{L}) \rightarrow \pi^*(\text{L})$
	3.6888	336.1	0.0170	(81%) HOMO-1→LUMO+3	$p\pi(\text{Cl}) \rightarrow \pi^*(\text{L})$